Study of the Kinetics, Mass Transfer, and Particle Morphology in the Production of High-Impact Polypropylene

P. KITTILSEN,[1] T. F. MCKENNA[2]

[1] Department of Chemical Engineering, Norwegian University of Science and Technology, 7491 Trondheim, Norway

[2] LCPP–Centre National de la Recherche Scientifique (CNRS)/ESCEP–Lyon, 43 Blvd. du 11 Novembre 1918, B.P. 2077, 69616 Villeurbanne Cedex, France

Received 10 March 2000; accepted 19 August 2000

ABSTRACT: A sequence of experimental steps was perfected to produce high-impact modified polypropylene (PP), and to study the influence of particle morphology and rubber content on the reaction kinetics, especially in terms of mass transfer limitations. It was found that after a critical copolymer content at approximately 40% (with respect to total weight), it was impossible to obtain high reaction rates. This is thought to be the result of a fundamental change in particle morphology attributed to the presence of a soft EPR copolymer phase in the micropores. © 2001 John Wiley & Sons, Inc. J Appl Polym Sci 82: 1047–1060, 2001

Key words: impact polypropylene; mass transfer; kinetics; Ziegler–Natta; polymerization

INTRODUCTION

To improve the impact strength of polypropylene (PP) one can incorporate a rubber copolymer phase, which is thought to absorb the mechanical energy from sudden shocks. This can be done either by mixing a PP homopolymer matrix with a rubbery compound [e.g., ethylene–propylene rubber (EPR)] in an extruder, or, as is more and more frequently the case, by producing this second rubbery phase directly inside the PP matrix. It is this second route to high-impact polypropylene (hiPP) that is investigated here.

Given the high volume of material produced, the production of hiPP is accomplished in a series of continuous reactors in a multistep process. As shown in Figure 1, a typical industrial process for the production of hiPP consists of an initial reactor(s) for the production of well-defined PP homopolymer particles, followed by a second step in which a copolymer of ethylene and propylene (around 1 : 1 mol fraction) is polymerized inside the same particles. The homopolymerization can be carried out either in the gas phase or in a polymer–liquid slurry with the liquid phase consisting of either a light hydrocarbon diluent (in sub- or supercritical conditions) or a liquid monomer. Because the copolymer is soluble in most hydrocarbons, the EPR stage is carried out in the gas phase.

The morphology of the final hiPP particles will obviously depend not only on the properties of the catalyst and on reaction conditions, much as is the case in homopolymerizations, but also on the amount of rubbery EPR copolymer formed during

Correspondence to: T. McKenna (mckenna@cpe.fr).

Contract grant sponsor: BRITE-EURAM; contract grant number: BE96-3022 (CATAPOL).

Journal of Applied Polymer Science, Vol. 82, 1047–1060 (2001)

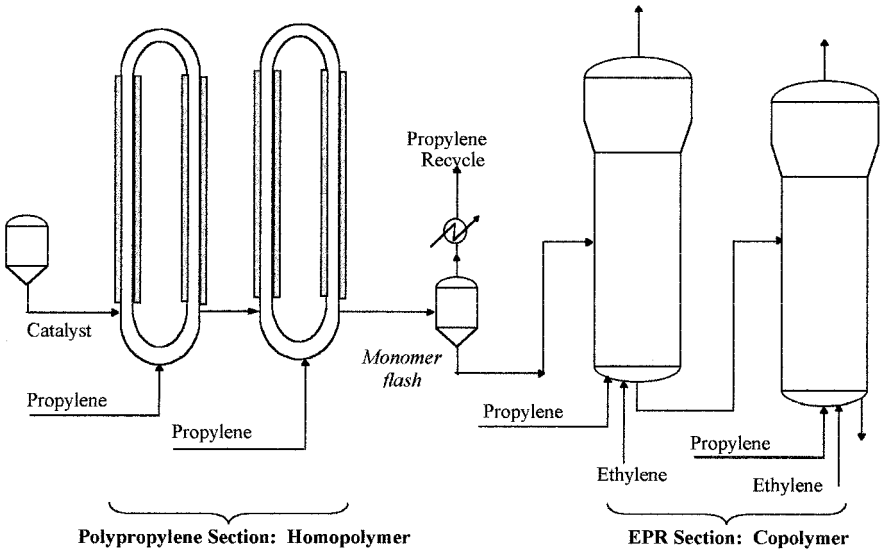

Figure 1 Spheripol process for hiPP. PP homopolymer is produced in bulk slurry in first reactor then fed to a second series of gas-phase FBR for copolymerization with ethylene in the gas phase.

the second stage. The copolymer is significantly more amorphous than is the more crystalline PP, and will therefore change the way particle size and morphology evolve. For instance, Kakugo et al.[1] studied the microstructure of hiPP particles with varying rubber content using scanning electron microscopy (SEM) and transmission electron microscopy (TEM). They found that at low EPR content, particle morphology was similar to that of the PP matrix (i.e., a continuous PP matrix consisting of an agglomeration of micrograins separated by a network of pores). However, as the EPR content was increased, the rubbery copolymer filled the interstices and, after approximately 50% EPR by total weight, they observed a sort of phase inversion, in which the particles appeared to be composed of a continuous EPR structure with PP in which micro- or mesograins were suspended.

Mass transfer limitations in homopolymerization were previously investigated by a number of authors, and it is generally agreed that if mass transfer limitations do indeed exist, their importance is strongly linked to the rate of polymerization, and will generally be significant only during the early stages of the polymerization.[2–4] However, given that there is definitely a relationship between the kinetics of olefin polymerization, mass transfer limitations, and the morphology of the growing particles, it is possible that the addition of a rubbery phase in the second stage fluidized bed reactors (FBRs) (shown in Fig. 1) might change the way in which the particles grow, and thus would have an influence on the rate at which monomer arrives at the active sites of the catalyst during the later stages of reaction. Initial work in this direction was undertaken by Debling et al.[5–7] In several investigations Debling and Ray[5,6] found that the particles they used maintained sufficient porosity to avoid any important mass transfer effects for most situations. At EPR contents of around 70% they observed that polymerization seems to take place only in the outer shell of the particles. It should be pointed out that the rates of polymerization they considered were in general somewhat lower than those one would encounter in an industrial situation.

Because it is desirable to use reaction rates that are as high as possible in industrial processes, we sought to determine whether similar observations could be made for higher rates of reaction in the current work. Of course, it is essential to avoid overheating of particles laced with EPR because the rubbery phase makes the particles sticky once it begins to form on the surface, and this tendency is exaggerated when the temperature increases. Nevertheless, as we show later, it is possible to obtain relatively high reaction rates, especially if one introduces a third reaction step for the gas phase of ethylene homopolymerization. This last step has the advantage of allowing us to significantly boost reaction

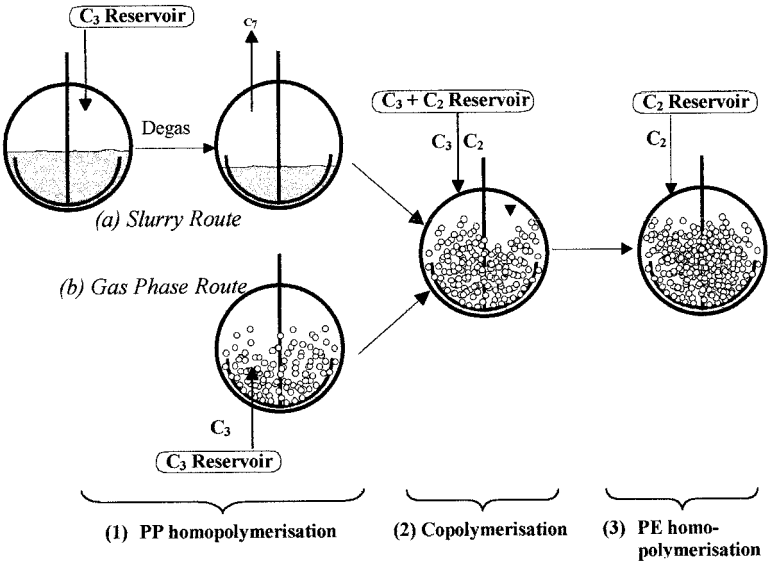

Figure 2 Experimental steps in the production of hiPP, and for the investigation of high-activity ethylene polymerization (optional last step).

rates in a short period of time in the same reactor, and therefore to easily explore the upper limits of mass transfer rates in EPR polymerization.

The objectives of the study are thus threefold: (1) to develop a reliable means of obtaining hiPP in a series of batch steps; (2) to explore the relationship between particle morphology and EPR content; and (3) to explore the relationship between particle morphology, mass transfer, and observed rates of reaction.

EXPERIMENTAL

Chemicals

The catalyst used in this study was commercial $MgCl_2$-supported $TiCl_4$ catalyst, with a mean particle diameter of approximately 30 μm. The triethyl aluminum (TEA) cocatalyst was obtained from Witco (Germany) and dissolved in heptane (Prolabo, France) to obtain the desired concentration. The electron donor used in the kinetic studies was cyclohexyl methyl dimethoxy silane (CHMDMS). The heptane solvent was a mixture of isomers dried on 3-Å molecular sieves. Propylene, ethylene, and hydrogen were purchased from Air Liquide (France). The purity of ethylene and hydrogen was >99.95%.

Reactor System

A high-pressure, 2.5-L spherical reactor used in all experiments is shown in Figure 2. The jacket temperature was maintained constant (i.e., isoperibolic operation) by water circulating from a thermostatted bath to the jacket of the reactor. Gas can be fed either from two ballasts or from external sources. A pressure reducer is used to control the pressure in the reactor. When needed, mixtures of propylene and ethylene were made by first filling a ballast with propylene to a certain pressure and then filling with ethylene. The partial pressures required for each monomer were calculated using the Soave–Redlich–Kwong equation of state (SRK–EOS).[8]

Production Procedure

The steps used in the production of hiPP are illustrated in Figure 2 and outlined below. The first two steps are followed by an optional third step for the homopolymerization of ethylene. As already mentioned the objective of this third step was to increase reaction rates as rapidly as possible, to investigate the possibility of mass transfer limitations associated with changes in particle morphology. The procedure listed here is the one found to be best and was used for all experiments presented in this work.

1. *Catalyst preparation for the gas phase of PP homopolymerization (step 1a).* Approximately 10 mg of catalyst was added to a small glass balloon along with 3 mL of a 0.3*M* TEA solution. A 20-μL sample of the electron donor (CHMDMS) was added 5

min later, and 1 min later just enough polymer charge was added so that it was just covered by the liquid. The solvent was evaporated under vacuum while the solution was stirred with a magnetic bar stirrer.

2. *Catalyst preparation for the slurry phase of PP homopolymerization (step 1b).* Approximately 300 mL of heptane was added to a large glass balloon, and TEA ($\sim$ 1*M*) was added to make 3 mM solution. Catalyst (10 mg) was added to a small glass balloon under argon, after which the catalyst was transferred to the large balloon by washing the small balloon with the heptane solution. Three minutes after the first contact between catalyst and the TEA solution, CHMDMS (5*M*) was added to make a 0.3-mM solution.
3. *Beginning of reaction.* The catalyst powder or solution was added (corresponds to time $t = 0$) with pressure of propylene slightly above atmospheric pressure and at low stirring rate ($\sim$ 50 rpm). This was done 15 min (gas) or 5 min (slurry) after the first contact between catalyst and TEA. About 200 cm^3 (STP) of H_2 was added. The stirring rate was increased (slurry: $\sim$ 550 rpm, gas: $\sim$ 250 rpm). The reactor temperature and pressure were then increased to desired levels (duration 4–5 min). The reaction was then allowed to progress to the desired extent.
4. *Transition from PP homopolymer to EPR.* (a) PP gas phase. The stirring rate was reduced to about 80 rpm. The reactor was degassed to 2.8 bar of propylene. (b) PP slurry phase. The stirring rate was reduced to about 80 rpm. The reactor was degassed and set under vacuum for about 20 min. The heptane was condensed using a cooling trap. The reactor was then filled with 2.8 bar of propylene.
5. *EPR stage.* The stirring rate was raised to about 280 rpm. The reactor was opened to the ballast containing an equimolar mixture of propylene and ethylene (see below for details). Reactor pressure was raised to 8 bar, thus bringing the gas-phase composition to the equilibrium value (gas phase mole fraction of ethylene, $x_E = 0.34$). See below for details on definition of equilibrium concentration.
6. *Transition from EPR stage to PE stage.* The stirring rate was decreased ($\sim$ 80 rpm) and the reactor cooled a few degrees. The reactor was degassed and vacuum applied until a pressure of 0.03 bar was reached. The stirring rate was then increased ($\sim$ 280 rpm) and the reactor was opened to the ballast with ethylene to reach the desired total pressure.
7. *End of experiment.* The reactor was cooled and degassed, then vacuum was applied until a reactor pressure of 0.03 bar was achieved. The reactor was filled with argon and opened once it was at room temperature.

The experimental conditions used in the runs discussed below are summarized in Table I.

Determination of Copolymerization Equilibrium Composition

Because it is important to maintain constant composition in the EPR phase, it was necessary to find a method that would allow this. Ideally, the reactors used in this type of study would be equipped with a control loop plus a gas chromatograph that could be used to ensure constant gas phase composition. Unfortunately, such a system is not available for the reactor described above, and it was necessary to find another means of doing so. If we correctly choose the composition of the gas phase we should immediately attain a pseudosteady state in the semibatch reactor that allows us to produce a copolymer with constant mole fraction of 0.5 ethylene and propylene.

Because it is impossible to know the relative reactivities of ethylene and propylene on the catalyst system *a priori,* it is necessary to experimentally determine the mole fraction of ethylene needed. In principle we want to find x_E (mole fraction of ethylene) in the gas phase of the reactor such that the values of x_E at the beginning and end of a copolymerization step will remain constant. If this is the case, and we feed the reactor with a 50/50 mol % mixture of ethylene and propylene, then the relative rates of consumption of both monomers remain equal and constant. The gas compositions in the reactor before and after EPR polymerizations of varying lengths and beginning with different ethylene compositions are listed in Table II. It appears that in each experiment, the ethylene mole fraction moves toward 0.34. For some cases starting with ethylene mole fractions below 0.34 this value was not reached because the experiment was stopped before this

Table I Experimental Conditions

Run	PP Media	PP Pressure (bar)	T_R (°C) (PP)	EPR Pressure (bar)	T_R (°C) (EPR)	% EPR (wrt total mass)	C_2 Pressure (bar)
P013	C_7 slurry	4	70	—	—	—	—
EPR027	Gas	8	60	8	60	30	—
EPR031	C_7 slurry	8	60	8	60	15	—
EPR046	C_7 slurry	8	60	—	—	—	8
EPR047	C_7 slurry	8	60	8	60	61	—
EPR048	C_7 slurry	8	60	8	60	39	8
EPR049	C_7 slurry	8	60	8	60	18	8
EPR051	C_7 slurry	8	60	8	60	28	8
EPR053	C_7 slurry	8	60	8	60	40	8
EPR054	C_7 slurry	8	60	8	60	34	—
EPR057	C_7 slurry	8	60	8	60	45	8
EPR058	C_7 slurry	8	60	8	60	50	8
EPR059	C_7 slurry	8	60	8	60	37	8

happened. Nevertheless, the composition at the end of the experiment increased over that of the initial value. Based on this, it is concluded that the equilibrium mole fraction of ethylene (giving an equimolar ethylene–propylene composition in the copolymer) is 0.34. Using a total pressure of 8 bar for EPR polymerization, it was calculated from SRK–EOS that the reactor should contain 2.8 bar at the end of the PP stage, before the pressure is increased to 8 bar with the 50/50 mol % mixture in the ballast to obtain an ethylene mole fraction of 0.34.

Calculation of Reaction Rate

When doing a three-step polymerization (PP, EPR, PE), three different ballasts would normally be needed to measure the reaction rate in each of the steps with a ballast method; however, the reactor is equipped with only two. Two different methods were therefore used to measure the reaction rate, one based on interrupting the monomer flow to the reactor and measuring the rate of pressure drop, and the other based on continuously monitoring the pressure in the ballast. The pressure drop in the reactor method was normally used for PP polymerizations (because we were less concerned about obtaining exact kinetic data in this stage), and the ballast method used for EPR and PE polymerizations.

The pressure-drop method is based on the idea that upon closing the monomer feed to the reactor, monomer will disappear as a result of the reaction and pressure will fall. There is thus a relation between pressure drop and reaction rate. Note that we used a slurry prepolymerization stage for the three-step processes, which means that when the reactor is filled with a solvent, this also must be taken into account to find the real reaction rate. The equilibrium between monomer in the gas phase and in the slurry phase is a little altered when the pressure drops. Using a mass balance over the reactor shows that, per mole of

Table II Start and End Mole Fractions of Ethylene in Reactor Gas Phase in EPR Step

Run	Cat	EPR Pressure (bar)	T_R (°C) (EPR)	% EPR (wrt total mass)	x_E Start	x_E End
EPR007	T1	8	60	70	0.16	0.29
EPR010	T1	8	60	49	0.25	0.34
EPR011	T1	8	60	29	0.17	0.23
EPR020	T1	8	60	45	0.34	0.34
EPR021	T1	8	60	30	0.34	0.34

monomer disappearing in the gas phase, about two moles of dissolved monomer disappear. The monomer concentration in the slurry was calculated using the SRK equation of state. Every 5–10 min, we measured the time it took for the pressure to fall 0.04 bar from the normal 8.00 bar (this took about 1 min). Note that the time required to obtain the desired pressure after injecting the catalyst is on the order of about 4–5 min. Also after this, it takes another 10 min before the reaction reaches its highest level. Data points for the homopolymer stage were taken every 5 min, giving activities at 10, 15, 20 min, and so on.

In the second method, continuous measurements of the monomer pressure in a ballast were interpreted using the SRK–EOS to obtain a continuous productivity (mass of polymer per gram of catalyst as a function of time). In our case, the pressure was recorded on an analog printer and the reaction rates were taken as the derivatives of the productivity curves.

Evaluation of Particle Morphology

Three methods were used to characterize the particle morphology: particle bulk density; Hg intrusion porosimetry; and a method based on image analysis.

The bulk density was measured by filling a 50-mL syringe to measure the bulk volume and weighing the polymer.

Analyzing the cut surface of particles for regions of polymer and pores can yield information about the porosity. Ideally, if one has a perfect cut (the polymer morphology is unchanged by the act of cutting) and analyzes enough surfaces, the area of polymer and the area of pore surface will correspond to the volume of polymer and pores in the sample. Thus an analysis of the cut surface of a few samples will give an idea of the porosity, in which the uncertainties are whether it is representative of the whole sample and whether the image analysis parameters are set correctly.

In this work, the particles were cut using a razor blade and SEM micrographs of these particles were taken. The cutting was done both at ambient temperature and after cooling the particles using liquid N_2, without any visible difference between the two conditions. Although microtoming the particles is probably a better way to ensure that no smearing of the cut face occurs, close investigation of these surfaces at high resolution showed little or no smearing, and because we were not looking for micropores and very fine features in this work, cutting with a sharp razor blade was deemed acceptable (and is faster). The images were scanned and digitally edited so that only the surface was left in the image. Each pixel in the image was assigned a value between 0 and 1, corresponding to the brightness of the pixel (0 = black, 1 = white). The scanned image was then transformed into an image with only two gray tones, one for pores and one for polymer. The black–white limit (or pore cutoff point) was set manually, so that the pores and polymer areas corresponded to the original one. This had to be done for each image because the images were exposed under different conditions, with varying degrees of darkness of the images. To find this color limit, a plot of the porosity as a function of limit factor f was made. The curve raised sharply near what we assumed to be the true value attributed to the sudden incorporating of the polymer into the porosity. At the optimal value of the cutoff point, the number of pore pixels compared to the total number of pixels in the surface yields the porosity. Admittedly, the image analysis method (IAM) did not give us the full porosity of the particle, because it is impossible to measure the contribution of small micropores. In addition, choosing the cutoff point that separates porous from nonporous zones was a delicate and somewhat subjective task. Nevertheless, there are two positive points that can be made for the IAM. First, it is a useful means of quantifying the radial variation of porosity inside well-cut particles. Second, we have found that by performing a series of initial Hg intrusion analyses, one can select a realistic value for the cutoff point. The method is demonstrated in Figure 3.

RESULTS AND DISCUSSION

Choice of PP Homopolymerization Step

The initial experimental runs were concerned with defining the PP step that produced the most regular, reproducible particles possible. This objective was defined to ensure that when we began to investigate the influence of EPR formation on particle morphology, any changes or anomalies encountered could clearly be attributed to this second step, and were not a result of irregularities that might occur during the PP homopolymerization. Typical morphologies of the PP homopolymers obtained with the catalyst tested here are shown in Figure 4. This dependence of the mor-

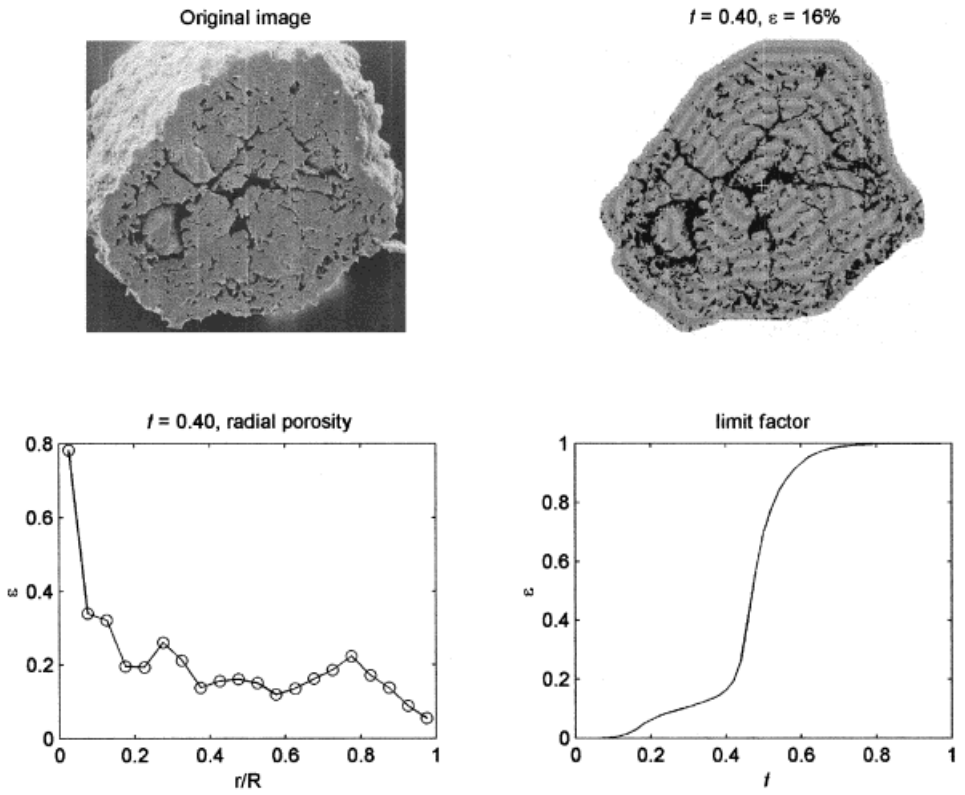

Figure 3 Porosity analysis of a PP-particle (P013). Gray tones are artifacts to illustrate separation of layers for analysis and have no physical meaning.

phology on the polymerization route chosen was 100% reproducible in all of the runs. Clearly, the initial polymerization step has a strong influence on the final particle morphology, with a more regular, spherical shape being obtained from the slurry polymerization. It has been pointed out by Pater et al.[9] that prepolymerization can have a significant influence on final particle morphology,

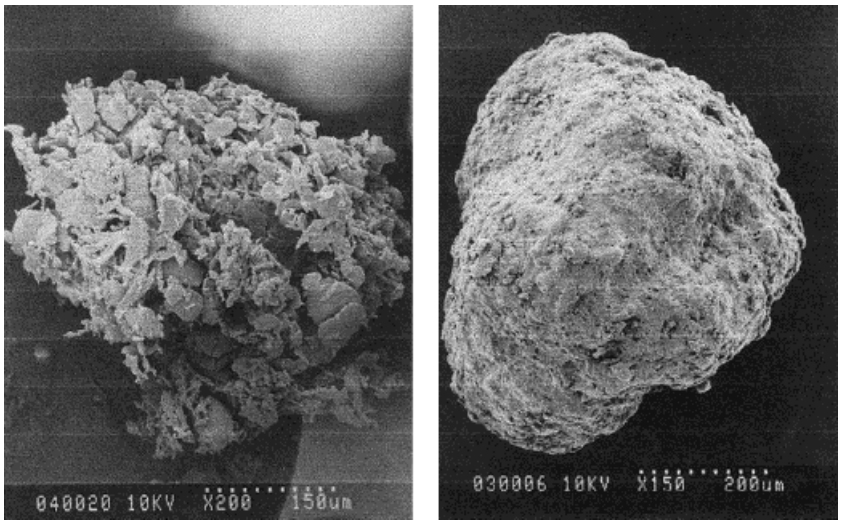

Figure 4 Representative particles from gas phase (left) and slurry (right) experiments.

and it might therefore be possible to obtain well-controlled morphologies in the gas phase with correct prepolymerization conditions. This aspect of particle growth is beyond the scope of the current work, and will be treated in a forthcoming study.

The fragmentation process that occurs is obviously different in the gas and slurry phases, and this might be in part the result not only of the presence of the solvent in the slurry reactions but also of better initial temperature control. It is possible that some overheating might occur in the gas phase. This, coupled with the swelling of the nascent polymer by small amounts of heptane, will lead to completely different conditions for the crystallization of the nascent polymer, and thus to different fragmentation behavior during the initial stages of the reaction. At this stage, of course, this is simply a hypothesis and will not be investigated further in this study.

Suffice to say that, although it is possible to use either type of particle shown in Figure 4 to make hiPP, it was decided to use the slurry route for the production of PP homopolymers, to avoid not only eventual problems linked to the fragile nature of gas-phase particles but also to problems of sticking that might arise. Initial studies showed that the particles produced in the gas phase led to more agglomeration and sticking than that observed in particles produced in the slurry phase. It is possible that the much higher exposed surface area of particles produced in the gas phase polymerization described here would be more susceptible to causing such problems.

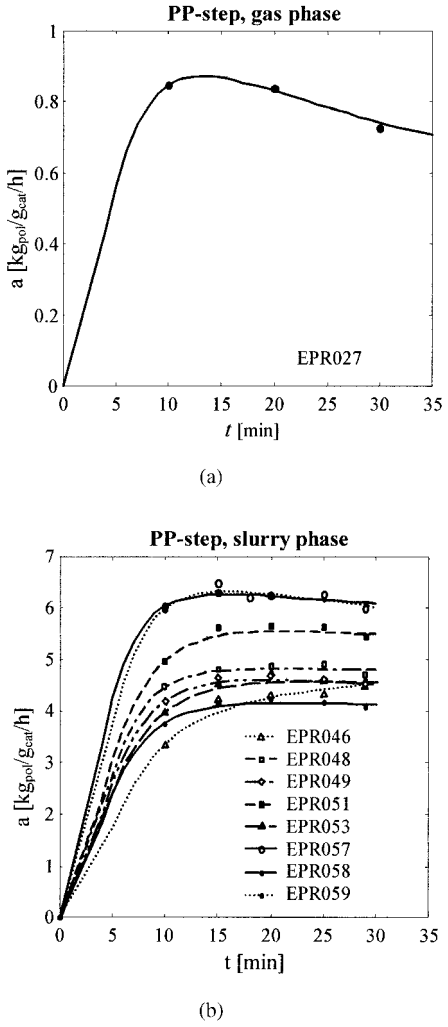

Figure 5 Rate curves for the homopolymerization of propylene in gas (a) and slurry (b) at 60°C.

Kinetics

The activation stage of the PP slurry-phase homopolymerizations can be attributed in part to the experimental procedure. Temperature and pressure are increased from 30 to 60°C and from 1 to 8 bar, respectively, over a period of about 5 min. As shown in Figure 5, the average activity for the PP homopolymerizations after 15 min was 5.1 kg (PP) g^{-1} (catalyst) h^{-1}, with a standard deviation of 0.9.

The rates of reaction for the copolymer step are shown in Figure 6. It can be seen that, despite the risks associated with the melting and increased stickiness of amorphous EPR, relatively high rates of polymerization can be obtained in this gas-phase reaction. These experiments were performed at 60°C (see Table I). Not shown in Figure 6 are a series of runs that were performed at 70°C. It was found that there was significant agglomeration, and occasionally even total agglomeration during the EPR stage at 70°C. For this reason, we limited the first two steps to a nominal temperature of 60°C. Much like the PP homopolymerizations shown in Figure 5, these reactions are characterized by a typical period of activation, followed by a relatively constant rate period. The activation phase of the second step lasts for significantly less time that that of the PP homopolymerization, and the constant rate is between two and four times that of the constant rate in the PP step. It is likely that the activation period is much shorter (and in fact corresponds more or less to the time for T and P to reach their steady-state values) because most them have already been activated during the PP stage, and there is no reason for us to expect that there would be any

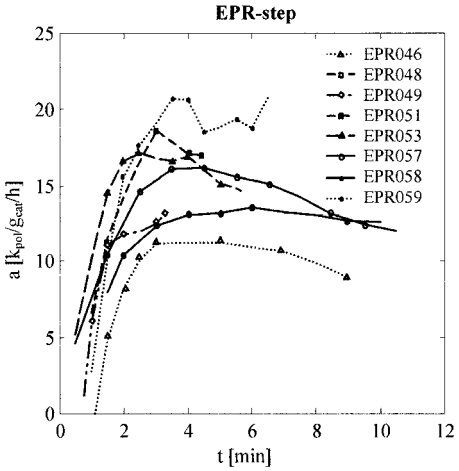

Figure 6 Rate curves for the production of hiPP (EPR phase) at 60°C.

measurable deactivation of the catalyst between the PP and EPR steps. The fact that the copolymerization activity is much higher is also to be expected. It is well known that ethylene is much more reactive than propylene, and that the presence of an α-olefin such as propylene has a synergistic effect on the rate of ethylene polymerization. In the PP stage, the reaction rate is sufficiently low that the reactor temperature remains close to the 60°C set point for most of the experiment. However, the higher rates in the EPR stage produce slight temperature increases, which, although definitely not zero, do not exceed 4 or 5°C.

As we mentioned earlier, a certain number of the hiPP runs were directly followed by an ethylene homopolymerization step, to examine the eventual influence of changing particle morphology on mass transfer resistance/polymerization kinetics. The results of these experiments can be seen in Figures 7 and 8. The rate curves [Fig. 7(a)] are clearly divided into two families: a group where peak activities between 60 and 100 kg of polymer per gram of catalyst per hour (kg g^{-1} h^{-1}) are observed during the first instants of the EPR stage, and a second family of experiments where the activities remain relatively low and are similar to those observed in the EPR stage. The average peak rate for the high activity runs was 86 ± 7 kg g^{-1} h^{-1}, and for the low activity runs it was 16 ± 1 kg g^{-1} h^{-1}. There is a significant exotherm in the experiments showing high peak activities, and the gas-phase temperature can increase by over 30°C in some cases [Fig. 7(b)]. Despite the large increase in temperature, the observed rates of polymerization in all EPR + PE experiments seem to tend toward the same final value. Catalyst deactivation, therefore, does not seem to be affected by (short) exposure to relatively high temperatures, and is thus probably chemically controlled.

The correlation between the value of peak activity and the quantity of EPR phase is shown in Figure 8. The result is rather striking and it appears that the presence (or absence) of an initial peak is strongly associated with the quantity of EPR contained in the hiPP particles. It is tempting to attribute this behavior to a number of factors. Increased temperature will obviously provoke an acceleration of the reaction rate, which in turns leads to higher temperatures, and so forth. However, this cannot be the only reason for the

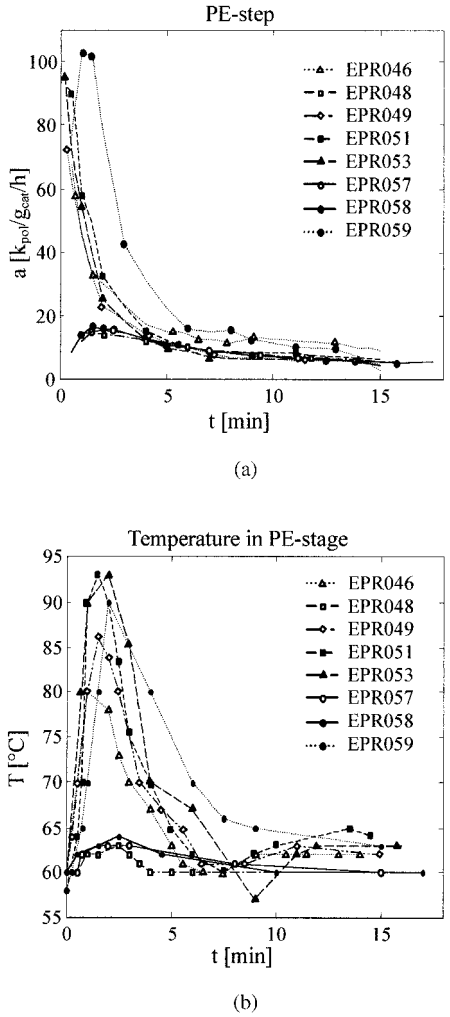

Figure 7 Rate curves for the optional third stage ethylene homopolymerization (a) and temperature profiles for the same reactions (b).

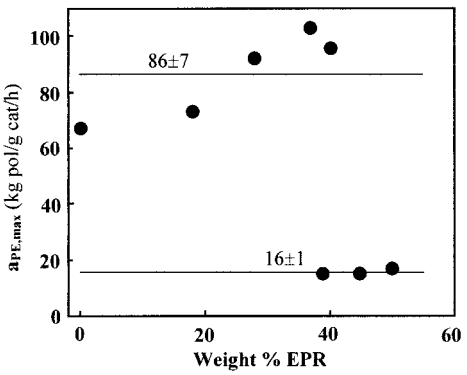

Figure 8 Peak activities for PE phase of three-step experiments as a function of % EPR in PP + EPR matrix.

difference between the two sets of experiments. First of all, even if temperature excursions can account for a part of the higher rates of reaction, there must be a physical event that sets off an exotherm. The reproducibility of the runs suggests that temperature increases cannot be attributed to variability in the functioning of the reactor.

To compare the two levels of peak activities on equal terms, the effect of temperature must be ruled out (i.e., we need to reduce the effect of the exotherm as much as possible). For this reason, we scaled the peak activities observed for the two families back to a reference temperature. The peak activity is normally reached slightly before the peak temperature (e.g., see Fig. 7) because of the heat transfer resistance from the interior of the reactor (the agitator + gas phase + polymer) to the reactor walls and jacket. The temperature at the height of the peak activities for the high activity runs is on the order of 70–80°C, and for the low activity runs it is on the order of 62–64°C. Using an Arrhenius-type temperature dependency and a value for the activation energy (E_A) of 45 kJ/mol, the average activities from the EPR stages of the two families of activity were rescaled to 60°C. The equivalent activities at 60°C are:

$$a_{\text{low}}^{60} = 14 \pm 1 \text{ kg g}^{-1} \text{ h}^{-1}$$

$$\text{and} \quad a_{\text{high}}^{60} = 43 \pm 6 \text{ kg g}^{-1} \text{ h}^{-1}$$

Therefore, one can probably conclude that, even if the increased temperature exacerbates the peak, there is definitely some kind of enhanced rate of reaction in the EPR stage for the hiPPs that contain less than 40 wt % EPR. Second, this cannot be a chemical effect resulting from the enhancement of ethylene polymerization attributed to the presence of propylene because, if it were, one would expect to find higher rates in the experiments with more EPR. The propylene concentrations would be slightly higher here, and one would therefore expect a slightly higher rate of ethylene production in these cases. In fact, the rapid deceleration of the reaction rate in the high-activity experiments can probably be attributed to a depletion of the residual propylene.

Because the rate of reaction is proportional to the concentration of monomer at the active sites, and therefore to the rate at which monomer arrives there, it is most likely that the difference in peak rates observed here is the result of mass transfer limitations caused by some sort of change in the internal particle morphology. In the event that there were some sort of mass transfer resistance in the hiPP particles, it would become difficult to replace the monomer that is consumed by the reaction, and the rate of polymerization would thus not increase. This type of behavior has been well documented for homopolymerizations.[1,3,10] The big difference between the reactions studied here and the homopolymerizations, insofar as mass transfer limitations are concerned, is that in the homopolymer case any mass transfer resistance will be encountered in fresh catalyst particles where the activity is high and the surface area of the particles is low. (Monomer consumption is proportional to the mass of catalyst, but mass transfer to the particles is proportional to the surface area. The surface area per mass of catalyst increases rapidly right after the beginning of the reaction and thus if there is mass transfer resistance, it disappears after a few minutes.) In the case of the hiPP particles, if the observed kinetic behavior is the result of mass transfer resistance, this occurs late the reaction, and must therefore be attributed to some kind of change of the characteristic length scale for diffusion, in other words, a change in internal particle morphology. That this is so is reinforced by the clear and sudden change in observed peak activity at 40 wt % EPR content.

Particle Morphology

Electron microscopy studies of the different powders were used to study overall particle morphology from a qualitative point of view, as well as for the estimation of the overall particle porosity and radially dependent porosity.

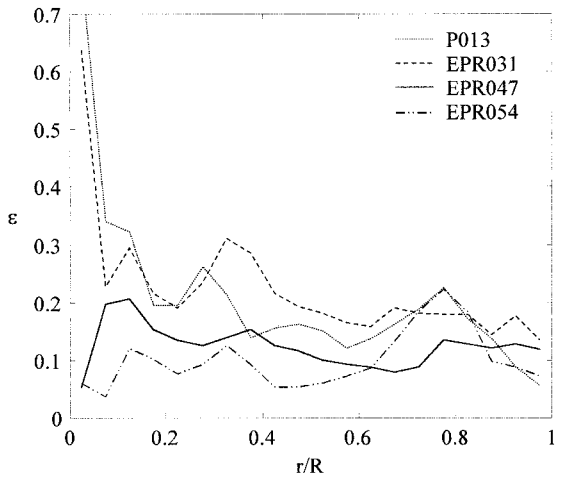

Figure 9 Porosity as a function of dimensionless radius for different samples. Values shown represent averages for one to three different photos per sample.

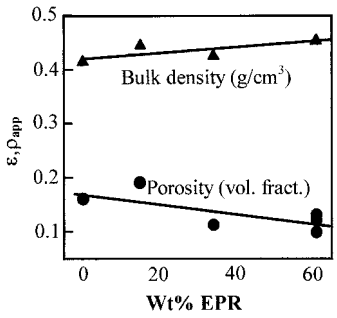

Figure 10 Porosity obtained by the image analysis method and bulk density as functions of EPR content.

From an extended study of cut particles, it seems that there is a radial variation in porosity, characterized by a type of core–shell structure, where the shell covers approximately 20–30% of the radius. This can be seen for almost all samples, regardless of the amount of EPR and transfer limitations. Figure 9 shows how the porosity varies as a function of radius for selected samples (radial variations were calculated using the IAM). Sometimes the core and the shell are almost separate phases, and it was not uncommon to find empty shells on some micrographs. There are several possibilities for this core and shell structure. (This point merits more attention and will be treated in a future publication from this group.) For the time being, for the study of the influence of EPR production on particle morphology, it is sufficient to have shown that the morphology at the end of the PP homopolymerization stage is reproducible, and we can thus safely say that any differences observed after the EPR (+ PE) stages are not the result of variation in the original matrix.

Bulk density measurements and the measurement of overall porosity as a function of EPR content are shown in Table III and Figure 10. In the IAM, it appears that the cut surface was slightly smeared by the razor blade in some instances (again, this is to be expected, especially with high EPR contents). This might cause some of the smaller pores to be obscured. However, it is clear that the larger pores stay intact; even if the IAM slightly underestimates the overall porosity, the micropores that might be obscured by the cutting process represent only a very small pore volume fraction, and the overall trend agrees very well with the bulk density and Hg intrusion results. The results of Table III and Figure 10 confirm that production of EPR in the PP particles can lead to a reduction in the overall porosity. Of

Table III Bulk Powder Characteristics

Powder	Mass % EPR (wt EPR + PP)	Mass % PE (wt EPR + PP + PE)	Bulk Density (g/cm³)	Porosity (Void Fraction)	
				Image Analysis[a]	Hg Intrusion
P013	0	0	0.415	0.16	—
EPR031	15	—	0.444	0.19	0.18
EPR054	34	—	0.425	0.11	—
EPR047	61	—	0.452	0.12	0.14
EPR048	39	24	0.435	0.16	—
EPR053	40	19	—	0.09	0.15

[a] The limit value for the discrimination between polymer and pores in the images was set individually, and varied from 0.3 to 0.5. Given value is an average of one to three samples.

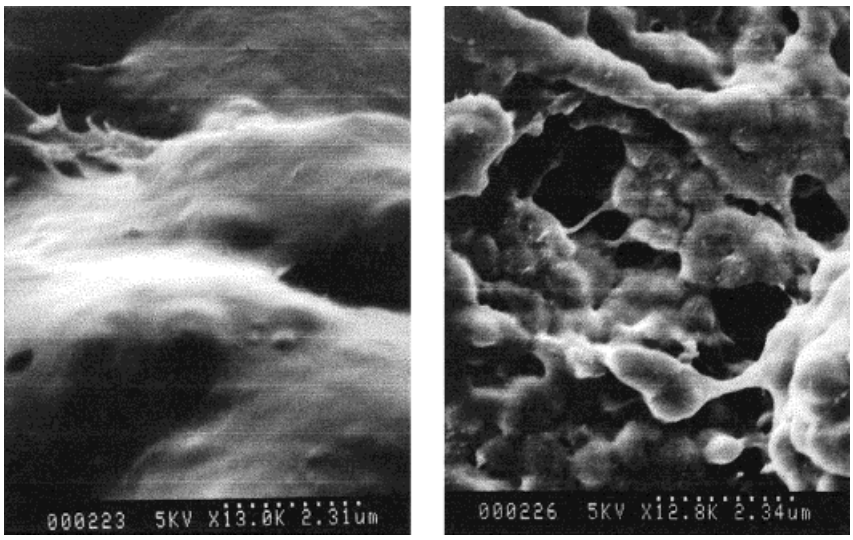

Figure 11 SEM pictures of particle surfaces from EPR031 (15 wt % EPR) at the same magnification. The left is an untreated particle and the right is a particle that was washed with heptane, dissolving the EPR.

course, this is to be expected, given the differences in the physical structure of PP and EPR phases.

The evolution of particle morphology in an impact PP reaction is commonly described as a two-step process. As mentioned earlier, at low EPR contents, the rubber is dispersed throughout the PP matrix in isolated domains, and a good portion of it can be found on pore surfaces throughout the particle. That this is the case can be seen in Figure 11, where SEM micrographs show two equivalent impact PP samples with an EPR weight fraction of 15%. Figure 11(a) shows a particle in the state in which it was found when it was taken out of the reactor, but not otherwise treated; Figure 11(b) shows a particle from the same batch that was washed in heptane. Because the EPR is soluble in heptane, most of the rubber domains found on particle surfaces will be removed in this process. We can clearly see that washing the particles in heptane changes the morphology of the particles. This implies that a good fraction of the EPR produced has made its way to the surface of the particle, and thus fills up a certain portion of the micro- and mesopores of the particles, and means that the EPR somehow seeps out of the PP matrix that is found immediately above the active sites.

The general trends of the evolution of particle morphology have been well documented by Debling et al.[5–7] Similar trends were observed in this work: a reduction of the microporous regions, with the growth of semicontinuous structures inside the hiPP particles. The major difference between the results presented here and those in the previously cited studies is that the catalysts and reactor conditions used in this work lead to the production of somewhat more porous particles, so that even at high EPR contents, our particles maintain a significant degree of macroporosity. As can be seen from Figure 12, the hiPP particles consisted of compact mesoparticles and almost unchanged macropores. The critical length scale for mass transport at the mesolevel will be greatly affected as we progress from pure PP particles to the case where the micro- and mesopores no longer form a network.

Kakugo et al.[1,11] found that little EPR stays in the microparticles, so most of the EPR made does not contribute to the growth of the microparticles, but rather fills the interstices between them. EPR gradually fills the micropores (between the micrograins) and the mesopores. Once the EPR content reaches a certain point, the meso- and micropores no longer make up a network, but are separated into small closed pores, making small gas cavities and PP polymer dispersed in the EPR polymer. It thus seems necessary to add an extra dimension to the particle morphology model proposed by Debling et al.[7] by incorporating the observations of Kakugo et al.[11] The compact particle model that they propose seems to describe the evolution of particle morphology fairly well. In this model, the EPR seeps out of the microparticles and fills the

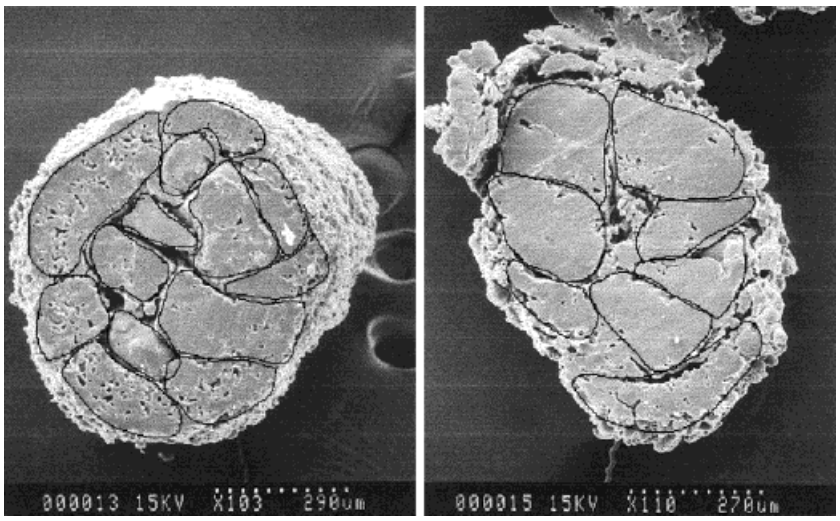

Figure 12 SEM pictures showing the mesoparticles in a polymer particle. The particles are from sample EPR047 (61 wt % EPR). What could be the mesoparticles are indicated. The diameter of the mesoparticles are typically 20–30% of the macroparticle diameter.

interstices of the growing polymer macroparticles, until the particles become more or less continuous at very high rubber content.

It seems that this model of particle morphology can help to justify the claim that the drop in activity seen in Figure 8 is attributed to mass transfer resistance. The resistance to monomer transport in the pores of a particle is most often low in a gas-phase reaction. To react, however, the monomer in the pores must diffuse through the polymer layer around the active sites. In the production of semicrystalline homo- and copolymers, the length scale that characterizes this step is not significant because of the network of pores that remain more or less intact during the reaction. However, EPR fills the pores and increases this diffusion length. Because the characteristic time for diffusion is defined as $\tau = l^2/D$ (where l is the characteristic length scale for diffusion and D is the effective diffusivity), small changes in the length scale for polymer diffusion can have significant repercussions on the rate of mass transfer. The SEM micrographs of cut hiPP particles shown in Figure 12 are clearly arranged in what we could call a mesoparticle structure. It is clear that the structures identified here are much larger than the microparticles identified in the classic multigrain model (MGM) model, but smaller than the overall particle, having diameters on the order of 20–30% of the overall particle size. If the diameter of these structures becomes the characteristic length scale for mass transfer, this could provoke moderate mass transfer resistance at high activities. It was previously reported in the literature that at high EPR contents (i.e., above 50% total weight), the copolymer phase becomes the continuous phase with PP fragments dispersed throughout.[5–7] This point coincides closely with the point where mass transfer resistance is encountered in the production of EPR particles. Further support of this idea comes from Debling,[5] who noted that particles containing on the order of 70% EPR are observed to be hollow. He reasonably attributes this to the fact that monomer simply cannot diffuse through the copolymer shell, thereby preventing any reaction in the particle center.

CONCLUSIONS

In the current investigation, we developed a simple series of steps to study the kinetics, particle morphology, and mass transfer resistance in the production of hiPP at moderate levels of activity. Study of particle morphology confirms the model for EPR formation on PP homopolymer particles: the EPR initially forms underneath the PP produced in the first stage of the reaction, and then seeps out to partially fill the micropores of the host matrix.

Kinetic studies of the third stage of ethylene homopolymerization suggest that this transfor-

mation of the internal morphology can provoke mass transfer resistance at high levels of activity for a moderate to high mass fraction of rubbery polymer, which here was found to be about 40%.

Portions of this work were financed by BRITE-EURAM project BE96-3022: CATAPOL.

REFERENCES

1. Kakugo, M.; Sadatoshi, H.; Sakai, J.; Yokoyama, M. in Catalytic Olefin Polymerisation; Keii, T.; Soga, K., Eds.; Elsevier: Amsterdam, 1990; pp. 345–354.
2. Floyd, S.; Choi, K. Y.; Taylor, T. W.; Ray, W. H. J Appl Polym Sci 1986a, 32, 2935.
3. Floyd, S.; Choi, K. Y.; Taylor, T. W.; Ray, W. H. J Appl Polym Sci 1986b, 31, 2231.
4. McKenna, T. F.; DuPuy, J.; Spitz, R. J Appl Polym Sci 1995, 57, 371.
5. Debling, J. A. Ph.D. Dissertation, University of Wisconsin–Madison, 1997.
6. Debling, J. A.; Ray, W. H. Ind Eng Chem Res 1995, 34, 3466.
7. Debling, J. A.; Zacca, J.; Ray, W. H. Chem Eng Sci 1997, 52, 1969.
8. Reid, R. C.; Prausnitz, J. M.; Poling, B. E. Properties of Gases and Liquids; McGraw-Hill: NewYork, 1987.
9. Pater, J. T. M.; Roos, P.; Weickert, G.; Westerterp, K. R. in Proceedings of the 6th International Workshop on Polymer Reaction Engineering; Dechema Monographien, 1998; Vol. 134, p. 103.
10. McKenna, T. F.; Barbotin, F.; Spitz, R. J Appl Polym Sci 1997, 62, 1835.
11. Kakugo, M.; Sadatoshi, H.; Sakai, J.; Yokoyama, M. Macromolecules 1989, 22, 3172.